

Direct observation of the magnetic polaron

Vyacheslav G. Storchak* and Oleg E. Parfenov

Russian Research Centre “Kurchatov Institute,” Kurchatov Sq. 1, Moscow 123182, Russia

Jess H. Brewer, Peter L. Russo, and Scott L. Stubbs

Department of Physics and Astronomy, University of British Columbia, Vancouver, British Columbia, Canada V6T 1Z1

Roger L. Lichti

Department of Physics, Texas Tech University, Lubbock, Texas 79409-1051, USA

Dmitry G. Eshchenko

Physik-Institut der Universität Zürich, CH-8057 Zürich, Switzerland and Swiss Muon Source, Paul Scherrer Institute, CH-5232 Villigen, Switzerland

Elvezio Morenzoni

Swiss Muon Source, Paul Scherrer Institute, CH-5232 Villigen, Switzerland

Tel'man G. Aminov

Institute for General and Inorganic Chemistry, Moscow 119991, Russia

Vladimir P. Zlomanov and Alexander A. Vinokurov

Department of Chemistry, Moscow State University, Moscow 119991, Russia

R. L. Kallaher and Stephan von Molnár

The Center for Materials Research and Technology, Florida State University, Tallahassee, Florida 32306, USA

(Received 19 March 2009; revised manuscript received 27 July 2009; published 16 December 2009)

Semiconductor electronics has so far been based on the transport of charge carriers while storage of information has mainly relied upon the collective interactions of spins. A new discipline known as spintronics proposes to exploit the strong mutual influence of magnetic and electrical properties in magnetic semiconductors, which promise new types of devices and computer technologies. The mechanism for such phenomena involves the concept of magnetic polarons—microscopic clouds of magnetization composed of charge carriers and neighboring magnetic ions—which determine most of the electrical, magnetic, and optical properties of the material. In spite of the importance of this quasiparticle, its observation remains a formidable challenge. Here we report that, using the positive muon as both a donor center and a local magnetic probe, we have been able to generate and detect the magnetic polaron and determine its size and magnetic moment in the magnetic semiconductor EuS.

DOI: [10.1103/PhysRevB.80.235203](https://doi.org/10.1103/PhysRevB.80.235203)

PACS number(s): 75.50.Pp, 72.25.Dc, 72.20.Jv, 76.75.+i

From the earliest transistor to the microprocessor in a modern computer, electronic devices have employed the transport of electric charge, which generates more and more heat as the conductors become smaller and smaller. Meanwhile, the spin of the electron also carries information whose transport need not generate Ohmic heating; this property could be exploited to enhance the multifunctionality of devices.^{1,2} Unfortunately, the semiconductors currently used in integrated circuits, such as Si, Ge, and GaAs, are nonmagnetic, so that the carrier's energy is almost independent of its spin direction. In contrast, in *magnetic semiconductors* (MS), the exchange interaction gives rise to pronounced spin-related phenomena.^{3,4} Extensive studies of MS in the 1960s and 1970s led to development of new concepts in condensed-matter physics such as magnetic polarons and magnetic phase separation. The current renaissance of interest in MS is caused in part by the fact that they are relatives to such materials as dilute magnetic semiconductors (DMS), high-

temperature superconductors and colossal magnetoresistance manganites.

An electron in the conduction band is normally a free carrier and thus contributes to the conductivity of the medium. To localize such an electron reduces this contribution but raises the electron's kinetic energy and is thus unlikely unless some local interaction lowers its energy at least as much. A familiar example is the attractive Coulomb potential of a positive donor ion. A less obvious example is the *exchange-energy* decrease when a number of magnetic ions with weak direct coupling experience a strong ferromagnetic (FM) coupling mediated by their exchange interactions with the aforementioned electron. Since this interaction increases with the local probability density of the electron, it favors localization and can be sufficient to *autolocalize* the electron into a FM “droplet” on the scale of the lattice spacing in an antiferromagnetic (AFM) or paramagnetic (PM) “sea.” This metastable quasiparticle is called a *magnetic polaron* (MP) (Refs. 3–6) and is of fundamental interest.

The MP concept has become the basis for any discussion concerning the physical properties of MS and related materials. Transport properties of these materials exhibit remarkable dependence on temperature and magnetic field: the resistivities of doped EuSe,⁷ EuS,⁸ or EuO with O vacancies⁹ change by 5–13 orders of magnitude in a narrow temperature range near the FM transition and magnetic fields of ~ 10 T suppress these resistivity maxima by 3–4 orders of magnitude (negative magnetoresistance). Measurements of both resistivity and Hall effect in the ferromagnetic spinel CdCr₂Se₄ clearly show that these remarkable properties reflect changes in the density, not the mobility, of charge carriers.^{3,4} Accordingly, the magnitude of these effects and their dependence on temperature and magnetic field cannot be explained in the framework of critical scattering^{10,11} but only in terms of electron localization into entities the size of a few unit cells—i.e., magnetic polarons. The complex formed by such an electron mediating an exchange interaction between nearest-neighbor ions is called^{5,6} a *giant spin molecule* since its magnetic moment is many Bohr magnetons. A somewhat larger MP (with weaker electron localization ~ 10 nm or more) was invoked to explain magnetic and transport properties in the II-VI (Ref. 12) and the III-V (Refs. 13–15) DMS.

Optical experiments in MS and DMS (Refs. 3, 4, and 16) also indicate bound MP formation, as do time-resolved magnetic measurements,¹⁷ including those in confined geometries¹⁸ and magnetic circular dichroism studies.¹⁹ The growing number of recent experiments which involve the concept of MP include studies of materials of current interest—two-dimensional electron systems, dilute magnetic oxides, cobaltites, etc. For a recent review see Ref. 20.

Although the overwhelming consensus leaves very little doubt about the existence of the MP, its direct observation remains a formidable challenge. Nevertheless, it is important to know its microscopic characteristics (binding energy, size, or magnetic moment) and to control them if possible as they determine the electrical and optical properties of the materials used as working media for prospective spintronics devices.

In order to find a way to detect the magnetic polaron directly, one has to appreciate the conditions for its formation: a specific feature of MS and related materials is strong dependence of the conduction electron energy on the magnetization of the crystal due to the *s-d* (or *s-f*) exchange interaction between the mobile carrier and localized spins, the minimal electron energy being achieved at the ferromagnetic ordering.^{3,4} For this reason the electron tends to establish and support this ordering. In the so-called free MP, the increase in the electron kinetic energy due to localization is assumed to be compensated by the *s-d* exchange energy gain upon transition from the PM (or AFM) to the FM state. This condition is, however, very stringent, as the gain in the exchange energy may be too small to localize the electron. In contrast, formation of an MP bound to a corresponding donor combines the long-range Coulomb interaction with the exchange coupling *J* to ensure localization of an electron with effective mass m^* so that the change in the free energy

$$\Delta F = \frac{\hbar^2}{2m^*R^2} - J\frac{a^3}{R^3} - \frac{e^2}{\epsilon R} \quad (1)$$

has a minimum as a function of *R*—the radius of the electron confinement.^{5,6} In order to compensate for the increase in the electron kinetic energy due to localization [first term in Eq. (1)] one needs an insulating matrix with low ϵ (to ensure a strong, unscreened Coulomb interaction) and a heavy electron which exhibits strong exchange coupling *J*. In the case of the FM semiconductor EuS ($m^* \approx m$, the free-electron mass; $\epsilon \approx 5$), rough estimates show that the first term (~ 1 eV) may be compensated by the combined effect of the exchange coupling [~ 0.5 eV (Refs. 3 and 4)] and the Coulomb attraction (*a* is the characteristic distance between nearest Eu ions). The exchange contribution to the localization amounts to a difference between the PM order of the host and the enhanced (FM) order in the MP. In an external magnetic field *H*, all Eu ions develop a net magnetization increasing toward low temperature; this reduces the energy advantage afforded by the exchange coupling, rendering the MP unstable at high *H* and low *T*. Therefore one has to search for the MP at high enough *T* that its mediated exchange contribution [the second term in Eq. (1)] is dominant.

The requirement of an insulating host can be met in pure EuS, which has a large enough energy gap (1.6 eV) to ensure exponentially low free electronic states even at room temperature. One can then *inject* a low concentration of free carriers into the empty conduction band from the ionization track of a high-energy positive muon (μ^+) which may then (after stopping) act as a center for electron localization²¹ to form the MP. The distinguishing feature of the present experiment using muons is that we follow the formation and behavior of a *single* MP in the sample; its interaction with any other MPs bound to possible impurities and defects can be safely ignored.

In a typical muon spin-relaxation (μ^+ SR) experiment, one accumulates a time spectrum of the individual μ^+ decay events that reveals the time-dependent spin polarization of initially 100% polarized positive muons stopped in the sample one at a time.^{22,23} Each incoming 4 MeV muon creates an ionization track of electrons and ions liberated during the μ^+ thermalization process. Experiments in insulating^{24–26} and semiconducting^{21,27–30} media have shown that the muon thermalizes very close (10^{-6} – 10^{-5} cm) to some of its ionization track products. Thus one of the excess electrons generated in the end of the track can be captured by the thermalized muon to form a muonium ($\text{Mu} \equiv \mu^+e^-$) atom (a light analog of the H atom where the proton is replaced by a positive muon). In semiconductors, this phenomenon of “delayed muonium formation” produces a model system with which to study electron capture by and release from the donor center (positive muon)²¹ in the extremely dilute limit: Mu (a neutral donor) is typically found at low temperatures while a diamagnetic bare μ^+ state (an ionized donor) is observed at higher temperatures.³¹

In semiconductors, two sets of quite different Mu states are so far known to coexist with diamagnetic state(s): deep (~ 0.2 eV or higher) Mu states with the characteristic hyperfine constants of $A \sim (0.1–0.5)A_{\text{vac}}$ ($A_{\text{vac}} = 4463$ MHz is the

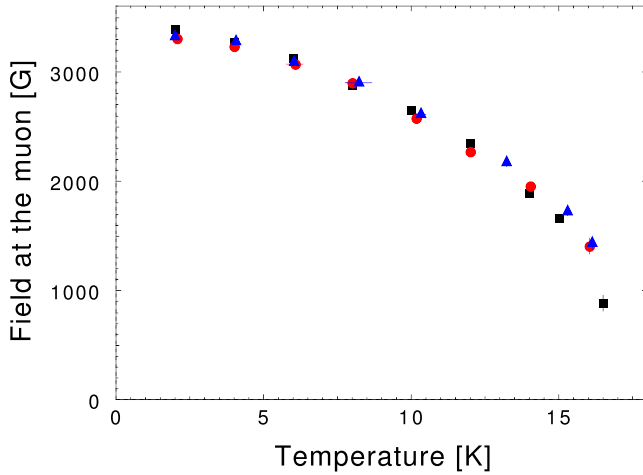


FIG. 1. (Color online) Local magnetic field B_μ at the muon in three different EuS samples under ZF (applied). Squares: the spherical polycrystalline EuS sample used in high magnetic field measurements (see below). Circles and triangles: disk-shaped polycrystalline EuS samples from different sources. The advantage of ZF- μ^+ SR over (e.g., bulk magnetization measurements) is that there need not be any net overall alignment of domains; moreover, since the muons stop randomly throughout the sample and the signal amplitude has an absolute calibration, observation of a single frequency rules out a mixture of phases. Clearly in this case the magnetic order is robust.

hyperfine constant for Mu or H in vacuum) found in Si, Ge, GaAs, etc.³¹ and shallow (~ 0.01 eV and $A \sim 10^{-4} A_{\text{vac}}$) Mu states detected in CdS, CdTe, ZnO etc.³²

In magnetic semiconductors, the second term in Eq. (1) may cause formation of a Mu bound state with an electron wave function more compact than in a typical Mu shallow donor state: the long-range Coulomb interaction ensures initial electron capture while the short-range exchange interaction provides further localization via formation of a magnetic polaron bound to the muon. Transverse magnetic field μ^+ SR techniques provide a reliable way to detect the MP thus formed and to determine its spectroscopic characteristics.

Time-differential μ^+ SR experiments were performed on the M15 surface muon channel at TRIUMF using the *HiTime* apparatus with a time bin size of 48.8 ps (the actual time resolution is ~ 150 ps). In order to get rid of demagnetization effects in applied magnetic fields^{22,23} we used a ball-shaped EuS powder sample 7 mm in diameter. Preliminary results on μ^+ SR studies of EuS with the aim to detect the magnetic polaron can be found elsewhere.³³

In zero magnetic field (ZF) we detected oscillations of the muon spin in the FM state. An important point here is that there is only one line (a single frequency) in the μ^+ SR spectra, which indicates that all muons occupy equivalent positions in EuS lattice. The internal magnetic field (B_μ) (see Fig. 1) thus measured at the muon in EuS at low temperature is typical of those measured by μ^+ SR in other FM materials,^{22,23} which suggests that the muon occupies an interstitial position in EuS. By analogy with other materials with NaCl structure, we assume this position to be tetrahedral,^{22,23} having four Eu ions as nearest neighbors. The ZF muon precession signal disappears above the FM

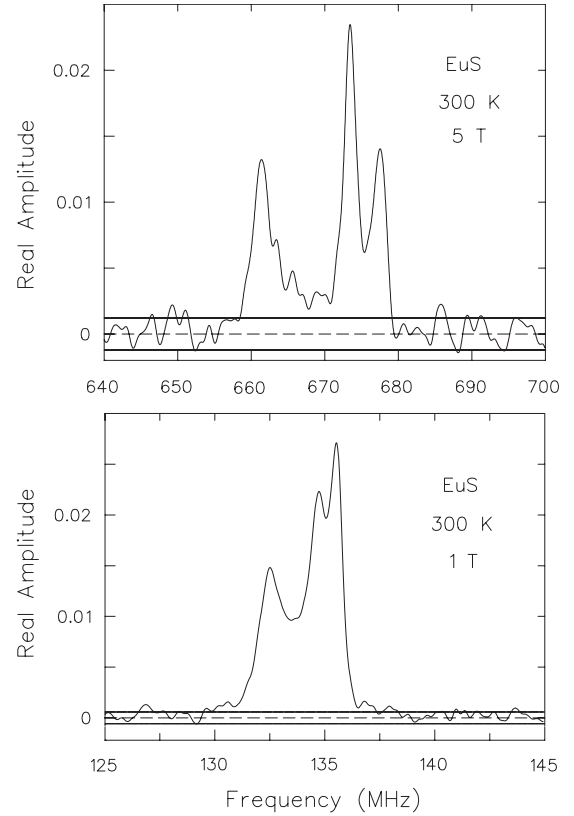


FIG. 2. Fourier transforms of the muon-spin-precession signal in EuS at $T=300$ K. Top: $H=5$ T; bottom: $H=1$ T. Such frequency spectra are routinely generated from high transverse magnetic field μ^+ SR time spectra in order to display the signatures of different states. In this case it is obvious that the central peak (associated with a bare muon) grows with increasing magnetic field (H) at the expense of two satellite peaks associated with the MP, indicating that bulk magnetization suppresses formation of the MP.

transition ($T_c \approx 17$ K) which is consistent with the disappearance of long-range FM order.

In transverse magnetic field (TF) with $H \gg B_\mu$, low-temperature measurements again detect a single line broadened due to interaction with Eu magnetic moments; this is the case both below and above T_c , up to ~ 100 K. At higher temperatures, however, the muon precession spectra split into three distinct lines (see Fig. 2). Evolution of these signals with magnetic field and temperature is presented in Figs. 2 and 3, respectively.

In TF- μ^+ SR—i.e., with the magnetic field \vec{H} applied perpendicular to the initial muon spin polarization—two classes of muon states can usually be distinguished by their characteristic precession signals: a diamagnetic, charged state (usually a bare μ^+) and paramagnetic, neutral state (usually a Mu atom). The former precesses at a frequency ν_μ (MHz) = $135.53879 B_\mu$ (T). In the limit of extremely weak magnetic field, the triplet (spin 1) state of Mu has a gyromagnetic ratio -102.88349 times that of the bare muon, thanks to the large electron moment coupled to the muon by the hyperfine interaction. At higher magnetic field, Mu precession splits into two lines according to the Breit-Rabi Hamiltonian,^{22,23} their separation determined by the muon-electron hyperfine con-

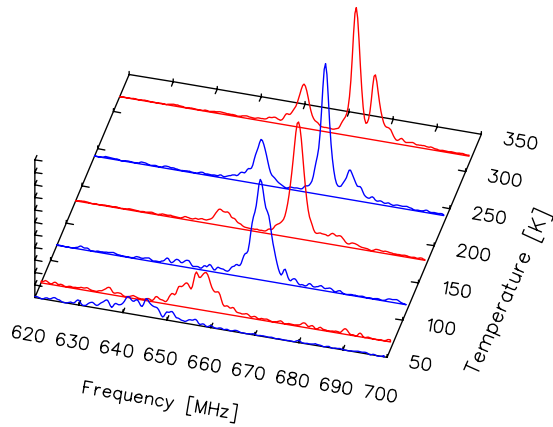


FIG. 3. (Color online) Fourier transforms of the muon-spin-precession signal in EuS in an external magnetic field of 5 T at different temperatures. As T decreases toward the Curie temperature ($T_c=16.5$ K), the bulk magnetization increases, broadening and shifting all three lines; but the magnetic polaron (satellite lines) is suppressed almost completely below 100 K.

stant A . In very high magnetic field the two observed Mu frequencies correspond to muon spin-flip transitions between states with the same electron-spin orientation. They appear symmetrically split by $\pm A/2$ about the diamagnetic frequency ν_μ . In semiconductors, weaker hyperfine interactions lead to smaller splittings (for shallow Mu states, *much* smaller) but the overall picture remains the same: the diamagnetic (bare μ^+) signal is represented by one central line (as for any spin $\frac{1}{2}$ particle in a magnetic field) and the two Mu lines appear on either side of it.³¹

We do see two lines split about a central one on Figs. 2 and 3. We claim that the central line is the signal from bare muons which avoid electron capture and that the two satellite lines represent muons that managed to capture and localize electrons to form the MP but the resulting paramagnetic spin system is far more interesting than a simple Mu atom. The localized electron spin is now strongly coupled (strength J) to neighboring Eu moments, forming a giant spin molecule of spin \mathcal{S} with the muon at its center. The electron spin also couples (strength $A \ll J$) to the μ^+ spin and thus transmits a hyperfine field to the muon. As always, the frequencies observed by μ^+ SR are associated with muon spin-flip transitions. Two satellite (MP) lines appear asymmetric with respect to the central line due to the ferromagnetic nature of the MP: local FM order creates a magnetic field shift with respect to the magnetic field acting on the muons which stay bare.

Figure 2 reflects the magnetic nature of electron localization: at higher magnetic field (5 T) increased magnetization diminishes the magnetic term in the free energy [see Eq. (1)], making it too small to compensate for the increase in electron kinetic energy due to localization. Accordingly, the amplitude of the central line is increased with respect to that of satellite lines when the magnetic field is increased from 1 to 5 T. In fact, this effect reflects effective electron *ionization* (magnetic polaron dissociation) in strong magnetic fields, known as the *boil-off effect*.³ Of course, this effect is never found in nonmagnetic semiconductors.³¹ In fact, in nonmag-

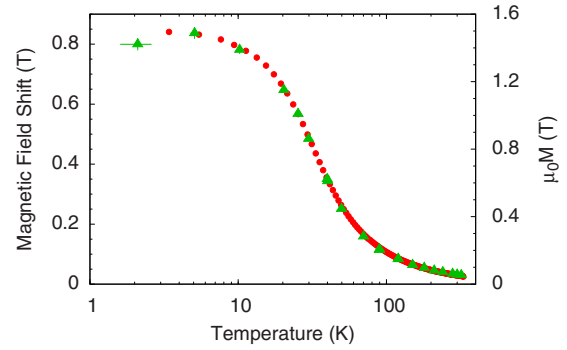


FIG. 4. (Color online) Temperature dependence of (a) the shift of the local magnetic field at the bare muon with respect to the applied magnetic field ($H=5$ T) in a EuS sphere (left vertical axis and triangles) and (b) the bulk magnetization of EuS measured by SQUID (right vertical axis and circles).

netic semiconductors, strong magnetic field has the opposite effect—magnetic freeze-out.³⁴ As the magnetization develops toward low temperature, all three lines exhibit enormous negative shifts (see Fig. 3) since the magnetic field at the muon follows bulk magnetization M : the temperature dependence of the central line shift is shown on Fig. 4 (left panel, triangles); the magnetization of our EuS sample measured by superconducting quantum interference device (SQUID) show similar behavior (Fig. 4, right panel, circles). Meanwhile the satellite lines disappear below about 90 K as the magnetic contribution to the electron localization diminishes [see Eq. (1)] and the MP no longer forms.

This behavior is in marked contrast with that of Mu in nonmagnetic semiconductors, where it disappears at *high* temperature.^{21,31} The difference is again because in magnetic semiconductors the electron is strongly coupled to a number of magnetic ions. This coupling is much greater than either the hyperfine interaction or the Zeeman splitting. This fact permits a simple model of Mu (MP) in EuS: one still (as in the case of Mu in nonmagnetic semiconductors) deals with the muon-electron system (two spin $\frac{1}{2}$ particles) but the electron spin is very strongly (through the exchange interaction) coupled with the Eu ions. This is because, by their very nature, the $4f$ levels of Eu ions are quite localized: $4f$ electrons in rare-earth chalcogenides are localized even more strongly than an electron in the ground state of a hydrogen atom. Therefore the density of the $4f$ electron wave functions of the Eu ions is negligible at the muon, allowing observation of the characteristic Mu-like two-frequency precession signal in high magnetic field. Furthermore, this strong exchange interaction J between the “muonium” (or MP) electron and the Eu ions produces a net MP spin $\vec{\mathcal{S}}$ (a big composite spin) which rapidly fluctuates (through orientational flips which change \mathcal{S}_z each time by ± 1) due to interaction with the spins of the nearest Eu ions outside the MP. Although the frequency of these fluctuations is about three orders of magnitude less than the characteristic fluctuation frequency ($\sim 10^{12}$ s⁻¹) of Eu spins in the paramagnetic state of EuS, it is still higher than the muon Zeeman frequency, which makes the mean-field approximation (MFA) valid in the entire temperature range where we see the MP. All these

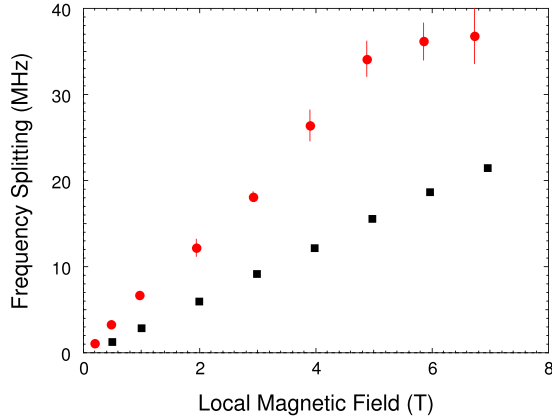


FIG. 5. (Color online) Magnetic field dependence of the frequency splitting between the two MP signals in EuS at $T=300$ K (squares) and $T=90$ K (circles). The splitting grows linearly with H in both cases but at low temperature the slope is steeper and the splitting saturates above 5 T. This H dependence is interpreted within mean-field theory [Eq. (2)] to give a hyperfine constant $A = 37 \pm 3$ MHz, a spin $S = 36 \pm 4$ and a radius $R \approx 0.3$ nm for the magnetic polaron at 90 K.

fluctuations do contribute to the MP lines splitting but they do not change the main spectroscopic signature—the characteristic two-frequency precession—arising from the fact that only the MP (Mu) electron has a significant density of its wave function at the muon. The model just outlined is discussed in detail in the Appendix.

The muon sees a mean-field proportional to the hyperfine coupling A and to the PM magnetization of the host. Then within the MFA, at low magnetic field and high temperature the splitting between the satellites can be expressed (see Appendix) as

$$\Delta\nu = A \left(\frac{g\mu_B B}{3k_B T} \right) (S + 1). \quad (2)$$

In high fields (though not high enough to decouple the electron and ions spins) and/or low temperatures, when the composite spin S is fully polarized, the satellite frequency splitting saturate at the value of A . This result seems to be model independent as it is the same as for any known Mu state with $A \ll A_{\text{vac}}$ at $B \gg A/\gamma_\mu$ in nonmagnetic semiconductors: both the deep Mu_{BC} state and the shallow Mu state exhibit satellite lines separated by $\pm \frac{1}{2}A$ from the central diamagnetic line.^{31,32} Although we failed to reach saturation in $\Delta\nu$ at room temperature, we found it at $T=90$ K above about 5 T (Fig. 5). From these measurements we determine $A = 37 \pm 3$ MHz.

This Mu state is fundamentally different from any previously studied isotropic Mu state found in insulators or semiconductors: its hyperfine constant is found to be about 100 times less than that of a deep Mu state and about 100 times larger than that of a shallow Mu state. Thus its electron wave function is significantly more compact than in a shallow state but considerably more dilated than in a deep state. For a Mu atom with $A \ll A_{\text{vac}}$ (with $R \gg R_{\text{vac}} = R_{\text{Bohr}} = 0.0529$ nm), the value of A scales as $1/R^3$, where R is the characteristic Bohr

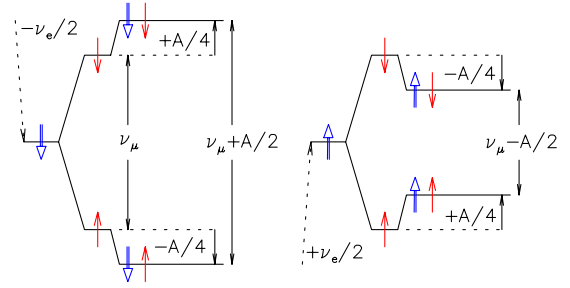


FIG. 6. (Color online) Energy-level diagram for an isotropic muonium atom in high magnetic field. Solid arrows (blue online) are electron spins and thin arrows (red online) are muon spins. The largest term in the spin Hamiltonian is the electron Zeeman splitting whose two levels (electron spin up and spin down) are shown separately. These are split by the muon Zeeman interaction and the resulting levels are shifted up or down by $A/4$ depending on whether the muon and electron spins are parallel or antiparallel, respectively.

radius of the corresponding $1s$ wave function. We find $R \approx 0.3$ nm, which is about six times larger than the Bohr radius of Mu (or H) in vacuum and about ten times smaller than that of a typical shallow state.

Fitting the linear part of Fig. 5 (the low magnetic field regime) with Eq. (2) we get $S = 36 \pm 4$. On the other hand, a simple estimate shows that a sphere of radius $R \approx 0.3$ nm around the muon in the tetrahedral interstitial position contains four Eu ions (the first coordination sphere), each having spin $7/2$, coupled by the Mu electron. When fully saturated this entity should present a composite spin of 14.5 (four Eu ions plus the Mu electron). The fact that we detected a magnetic polaron with composite spin significantly higher than the fully saturated value is consistent with the model of a saturated MP nucleus and unsaturated “region of enhanced magnetic moment” around it.³⁵ Formation of similar MP states is found in another magnetic semiconductor SmS (Ref. 36) and in the quasi-one-dimensional antiferromagnet LiCu_2O_2 .³⁷

In conclusion, using the positive muon as a donor center we have detected an individual MP bound to the muon in EuS. The characteristic radius and the composite spin of this MP at $T=90$ K are $R \approx 0.3$ nm and $S = 36 \pm 4$, respectively. This is consistent with MP composed of the four saturated nearest Eu ions surrounded by the region of the enhanced magnetic moment and an electron coupled to them so that this MP behaves as one entity.

ACKNOWLEDGMENTS

This work was supported by the Kurchatov Institute, the Canadian Institute for Advanced Research, the Natural Sciences and Engineering Research Council of Canada and the U.S. Department of Energy (Grant DE-SC0001769).

APPENDIX: SPECTROSCOPY OF A MAGNETIC POLARON BOUND TO A MUON IN A PARAMAGNET [DERIVATION OF EQ. (2)]

The spin Hamiltonian for an isolated muonium (Mu) atom (μ^+e^-) has the general form

$$\mathcal{H}/h = \vec{\mathbf{i}} \cdot \mathbf{A} \cdot \vec{\mathbf{s}} + \nu_e s_z - \nu_\mu i_z, \quad (\text{A1})$$

where $\vec{\mathbf{i}}$ is the muon spin, $\vec{\mathbf{s}}$ is the electron spin and the hyperfine interaction between them is in general represented by a tensor \mathbf{A} . The electron and muon Zeeman terms have been expressed in terms of their respective Larmor frequencies in the applied magnetic field $\vec{\mathbf{H}} = H\hat{z}$

$$\nu_e = g_e \mu_B H / 2h \quad \text{and} \quad \nu_\mu = g_\mu \mu_\mu H / 2h. \quad (\text{A2})$$

If the electronic wave function Ψ_e has the character of an s orbital, the hyperfine interaction is isotropic and can be simplified to

$$\mathcal{H}_{\text{hf}}/h = A(\vec{\mathbf{i}} \cdot \vec{\mathbf{s}}), \quad (\text{A3})$$

where A is a scalar³¹

$$hA = \frac{8\pi}{3} g_\mu \mu_\mu g_e \mu_B |\Psi_e(0)|^2. \quad (\text{A4})$$

In high transverse magnetic field $\nu_e \gg A$ (Paschen-Bach limit) the observed TF- μ^+ SR frequencies correspond to two muon spin-flip transitions with $\Delta m_s = 0$

$$\nu_\pm = \nu_\mu \pm \frac{A}{2} \quad \text{so that} \quad \Delta\nu \equiv \nu_+ - \nu_- = A, \quad (\text{A5})$$

as can be seen from the energy-level diagram shown in Fig. 6.

In magnetic semiconductors, the spin-polaron effect leads to a renormalization of the hyperfine interaction parameter A . Here two effects are important: (1) Additional electron localization due to a strong exchange interaction can cause an increase in the probability density $\Psi_e(0)$ of the electron wave function at the muon; in spherical symmetry this can be approximated by scaling A as $1/R^3$, where R is the mean radius of $\Psi_e(r)$. (2) Under certain circumstances, the strong exchange interaction between the Mu electron and nearby magnetic ions can lead to a qualitative change in its effective hyperfine interaction with the muon. To explain how this happens we must first discuss the phenomenology of the MP as a small FM droplet with spin \mathcal{S} and its own dynamics within the limits of MFA.³⁸

In magnetic semiconductors, the exchange interaction J between the magnetic ions and the carrier (in this case the Mu electron) is much stronger than any other interactions due to molecular fields, spin-orbit interactions, magnetic anisotropy contributions, etc. For this reason, both the electron spin and the spins of the FM-coupled magnetic ions are always collinear with the magnetic moment $\vec{\mathbf{M}}$ of the MP. Since $\mathcal{M} \equiv \langle \mathcal{M}_z \rangle \propto \langle \mathcal{S}_z \rangle$, where $\langle \mathcal{S}_z \rangle$ is the effective spin projection of the MP, we can write

$$\langle s_z \rangle = C \langle \mathcal{S}_z \rangle, \quad (\text{A6})$$

where C is a scalar constant.

The spin Hamiltonian for the polaron-plus muon is thus

$$\mathcal{H} = \mathcal{H}_{\text{MP}} + \mathcal{H}_\mu + j_{\text{an}}(\vec{\mathbf{S}} \cdot \hat{\mathbf{n}}), \quad (\text{A7})$$

where the terms are written in order of decreasing strength

$$\mathcal{H}_{\text{MP}} = J(\vec{\mathbf{s}} \cdot \vec{\mathbf{S}}) + h\nu_{\text{MP}}\mathcal{S}_z + h\nu_e s_z, \quad (\text{A8})$$

where J is the (huge) exchange coupling of the Mu electron with the surrounding Eu moments that comprise the FM droplet of spin $\vec{\mathbf{S}}$ and $\nu_{\text{MP}} \sim \nu_e$. The muon ‘‘sees’’ only the magnetic field H and the Mu electron’s hyperfine coupling A

$$\mathcal{H}_\mu = -h\nu_\mu i_z + hA(\vec{\mathbf{i}} \cdot \vec{\mathbf{s}}). \quad (\text{A9})$$

The magnetic anisotropy term (characterized by a constant j_{an} with a preferred direction $\hat{\mathbf{n}}$) is very small in Eu chalcogenides.⁴ When $k_B T > \mathcal{S}j_{\text{an}}$, thermal fluctuations cause a sort of Brownian motion of the orientation of a magnetic polarons net moment $\vec{\mathbf{M}}$ among $2\mathcal{S}+1$ quantum states of different \mathcal{S}_z , each of which has a fixed ratio of $s_z = +1/2$ and $s_z = -1/2$ amplitudes because the orientation of the electron spin is ‘‘locked’’ to that of the polaron spin $\vec{\mathbf{S}}$. Another way of looking at this is to first solve for the eigenstates of \mathcal{H}_{MP} and then treat the effect of \mathcal{H}_μ (neglecting j_{an}) as a perturbation mixing these eigenstates.

If the characteristic time τ_c of such fluctuations of \mathcal{S}_z is shorter than the period $1/\nu_\mu$ of muon precession then we are justified in using the MFA to replace the electron-spin operator by its average value, $s_z \rightarrow \langle s_z \rangle$, giving muon transition frequencies

$$\nu_\pm = \nu_\mu \pm \frac{A}{2} \langle s_z \rangle. \quad (\text{A10})$$

Such fast fluctuations can be expected if $k_B T \gg h\nu_\mu$, which thus defines the high- T regime when $\mathcal{S}j_{\text{an}}$ is negligible. The characteristic time required to sample all $2\mathcal{S}+1$ states of \mathcal{S}_z can be estimated as³⁹

$$\tau_c = (2\mathcal{S}+1)^2 \tau_0, \quad (\text{A11})$$

where τ_0 is the mean time between individual $\Delta\mathcal{S}_z = \pm 1$ transitions. In EuS, as in any rare-earth chalcogenide, $\tau_0 \sim 10^{12} \text{ s}^{-1}$ (Ref. 4) which determines $\tau_c \sim 10^9 \text{ s}^{-1}$.

At high T and low H we expect $\langle s_z \rangle \rightarrow 0$ so that the average electron spin ‘‘seen’’ by the muon (via the hyperfine interaction) is close to zero and the two lines ν_\pm merge. A perfect example of this is seen in SmS at high T .³⁶ To see ν_\pm split by the intrinsic hyperfine splitting A , one has to raise the magnetic field to satisfy the condition $g_\mu \mu_\mu H_{\text{eff}} > hA$, where $H_{\text{eff}} = H + \gamma\mathcal{M}$ is the effective field in the sample, H is the external magnetic field, \mathcal{M} is the bulk magnetization of the sample, and γ is a parameter of the molecular (Weiss) field³⁸ which also decouples the polaron spin \mathcal{S} from the Eu spins.

At low temperature and high field ($\mathcal{M}_0 H_{\text{eff}} > k_B T$) the fluctuations of the polaron spin settle down and its saturation magnetization \mathcal{M}_0 aligns with the external field

$$\langle \mathcal{M} \rangle = g_e \mu_B \langle \mathcal{S}_z \rangle \rightarrow \mathcal{M}_0 = g_e \mu_B \mathcal{S} \quad (\text{A12})$$

so that $\langle s_z \rangle$ saturates at $C\mathcal{S} = 1/2$, giving

$$\langle s_z \rangle = \frac{1}{2} \frac{\langle \mathcal{S}_z \rangle}{\mathcal{S}}. \quad (\text{A13})$$

In the PM phase where $T \gg T_c$ and $H_{\text{eff}} \approx H$, we get

$$\langle S_z \rangle = \mathcal{S} \mathcal{B} \left(\frac{g_e \mu_B \mathcal{S} H}{k_B T} \right), \quad (\text{A14})$$

where $\mathcal{B}(x)$ is a Brillouin function.³⁸

At high enough T so that $k_B T \gg \mathcal{M}_0 H$, according to the Curie law

$$\langle S_z \rangle = \mathcal{S}(\mathcal{S} + 1) \frac{g_e \mu_B H}{3k_B T}. \quad (\text{A15})$$

Then the eigenvalues are

$$\nu_{\pm} = \nu_{\mu} \pm \frac{A}{2}(\mathcal{S} + 1) \frac{g_e \mu_B H}{3k_B T}, \quad (\text{A16})$$

which corresponds to the characteristic splittings at high T ($k_B T \gg \mathcal{M}_0 H$)

$$\Delta \nu \equiv \nu_+ - \nu_- = A(\mathcal{S} + 1) \frac{g_e \mu_B H}{3k_B T} \quad (\text{A17})$$

and at low T ($k_B T < \mathcal{M}_0 H$)

$$\Delta \nu \equiv \nu_+ - \nu_- = A, \quad (\text{A18})$$

respectively.

*mussr@triumf.ca

¹S. A. Wolf, D. D. Awschalom, R. A. Buhrman, J. M. Daughton, S. von Molnár, M. L. Roukes, A. Y. Chtchelkanova, and D. M. Treger, *Science* **294**, 1488 (2001).

²G. A. Prinz, *Science* **282**, 1660 (1998).

³*Diluted Magnetic Semiconductors in Semiconductors and Semimetals*, edited by J. K. Furdyna and J. Kossut (Academic, New York, 1988).

⁴E. L. Nagaev, *Magnetic Semiconductors* (Imperial College, London, 2002).

⁵T. Kasuya and A. Yanase, *Rev. Mod. Phys.* **40**, 684 (1968).

⁶T. Kasuya, A. Yanase, and T. Takeda, *Solid State Commun.* **8**, 1543 (1970).

⁷S. von Molnár and S. Methfessel, *J. Appl. Phys.* **38**, 959 (1967).

⁸S. Methfessel and D. C. Mattis, *Magnetic Semiconductors*, edited by S. V. Vonsovskii (Mir, Moscow, 1972) (in Russian).

⁹G. Petrich, S. von Molnár, and T. Penny, *Phys. Rev. Lett.* **26**, 885 (1971).

¹⁰P. De Gennes and J. Friedel, *J. Phys. Chem. Solids* **4**, 71 (1958).

¹¹M. E. Fisher and J. S. Langer, *Phys. Rev. Lett.* **20**, 665 (1968).

¹²M. Sawicki, T. Dietl, J. Kossut, J. Igalson, T. Wojtowicz, and W. Plesiewicz, *Phys. Rev. Lett.* **56**, 508 (1986).

¹³H. Ohno, H. Munekata, T. Penny, S. von Molnár, and L. L. Chang, *Phys. Rev. Lett.* **68**, 2664 (1992).

¹⁴H. Ohno, *Science* **281**, 951 (1998).

¹⁵A. Kaminski and S. Das Sarma, *Phys. Rev. Lett.* **88**, 247202 (2002).

¹⁶G. Busch, P. Streit, and P. Wachter, *Solid State Commun.* **8**, 1759 (1970).

¹⁷D. D. Awschalom, J. Warnock, and S. von Molnár, *Phys. Rev. Lett.* **58**, 812 (1987).

¹⁸D. D. Awschalom, M. R. Freeman, N. Samarth, H. Luo, and J. K. Furdyna, *Phys. Rev. Lett.* **66**, 1212 (1991).

¹⁹B. Beschoten, P. A. Crowell, I. Malajovich, D. D. Awschalom, F. Matsukura, A. Chen, and H. Ohno, *Phys. Rev. Lett.* **83**, 3073 (1999).

²⁰S. von Molnár and P. A. Stampe, in *Handbook of Magnetism and Advanced Magnetic Materials*, Spintronics and Magneto-electronics, edited by Helmut Kronmüller and Stuart Parkin (John Wiley & Sons, Hoboken, New Jersey, 2007), Vol. 5.

²¹V. G. Storchak, D. G. Eshchenko, and J. H. Brewer, *J. Phys.: Condens. Matter* **16**, S4761 (2004).

²²A. Schenck, *Muon Spin Rotation: Principles and Applications in Solid State Physics* (Adam Hilger, Bristol, 1986).

²³J. H. Brewer, *Encyclopedia of Applied Physics* (VCH, New York, 1994), Vol. 11, p. 23.

²⁴V. G. Storchak, J. H. Brewer, and G. D. Morris, *Phys. Rev. Lett.* **75**, 2384 (1995).

²⁵V. G. Storchak, D. G. Eschenko, J. H. Brewer, G. D. Morris, S. P. Cottrell, and S. F. J. Cox, *Phys. Rev. Lett.* **85**, 166 (2000).

²⁶D. G. Eshchenko, V. G. Storchak, J. H. Brewer, G. D. Morris, S. P. Cottrell, and S. F. J. Cox, *Phys. Rev. B* **66**, 035105 (2002).

²⁷V. G. Storchak, S. F. J. Cox, S. P. Cottrell, J. H. Brewer, G. D. Morris, D. J. Arseneau, and B. Hitti, *Phys. Rev. Lett.* **78**, 2835 (1997).

²⁸D. G. Eshchenko, V. G. Storchak, J. H. Brewer, and R. L. Lichti, *Phys. Rev. Lett.* **89**, 226601 (2002).

²⁹V. G. Storchak, D. G. Eshchenko, R. L. Lichti, and J. H. Brewer, *Phys. Rev. B* **67**, 121201 (2003).

³⁰D. G. Eshchenko, V. G. Storchak, S. P. Cottrell, and S. F. J. Cox, *Phys. Rev. B* **68**, 073201 (2003).

³¹B. D. Patterson, *Rev. Mod. Phys.* **60**, 69 (1988).

³²J. M. Gil, H. V. Alberto, R. C. Vilao, J. Piroto Duarte, N. Ayres de Campos, A. Weidinger, J. Krauser, E. A. Davis, S. P. Cottrell, and S. F. J. Cox, *Phys. Rev. B* **64**, 075205 (2001).

³³V. G. Storchak, O. E. Parfenov, J. H. Brewer, P. L. Russo, S. L. Stubbs, R. L. Lichti, D. G. Eshchenko, E. Morenzoni, T. G. Aminov, V. P. Zlomanov, A. A. Vinokurov, R. L. Kallaher, and S. von Molnár, *Physica B (Amsterdam)* **404**, 896 (2009).

³⁴V. G. Storchak, D. G. Eshchenko, J. H. Brewer, B. Hitti, R. L. Lichti, and B. A. Aronson, *Phys. Rev. B* **71**, 113202 (2005).

³⁵A. Mauger and D. L. Mills, *Phys. Rev. B* **31**, 8024 (1985).

³⁶V. G. Storchak, J. H. Brewer, D. J. Arseneau, S. L. Stubbs, O. E. Parfenov, D. G. Eshchenko, E. Morenzoni, and T. G. Aminov, *Phys. Rev. B* **79**, 193205 (2009).

³⁷V. G. Storchak, J. H. Brewer, D. J. Arseneau, S. L. Stubbs, O. E. Parfenov, D. G. Eshchenko and A. A. Bush, *Phys. Rev. B* **79**, 220406(R) (2009).

³⁸J. S. Smart, *Effective Field Theories of Magnetism* (W. B. Saunders, Philadelphia, London, 1966).

³⁹D. Budker, D. F. Kimball, and D. P. DeMille, *Atomic Physics: An Exploration Through Problems and Solutions* (Oxford University Press, Oxford, 2003).